

# High Average Power Pulsed CO<sub>2</sub> Laser for Short Wavelength Light Sources

Akira Endo

*Research Institute for Science and Engineering, Waseda University, Tokyo  
Japan*

## 1. Introduction

### 1.1 Background of the emerging technology

Increase of average power of pulsed CO<sub>2</sub> laser was required by strong demand of the semiconductor industry, in pursue of the next generation of lithography light source at 13.5nm (Endo, et.al, 2006). The target average EUV power was increased from 10W level in the beginning to several 100W levels in the recent maturing period. No existing solid state laser technology satisfies the demand of the average power as the laser driver, by counting the laser-EUV conversion efficiency around 1%. Intensive research of one decade also showed that opacity, namely self absorption of the generated EUV light is less significant in high Z plasma, driven by a longer wavelength laser. CO<sub>2</sub> laser produced Tin plasma showed more than 4% conversion efficiency in practical target geometry. Details are recently reviewed by A.Endo (Endo, 2010) and V.Y.Banine (Banine et.al, 2011). Interested readers are advised to refer to these articles. The established architecture is shown in Fig.1 as the laser produced Tin plasma which is generated from mist target of 300 $\mu$ m diameter, irradiated by 15ns CO<sub>2</sub> laser pulse. The mist target is produced from a 10 $\mu$ m Tin droplet after irradiation by a solid state laser with smaller pulse energy.

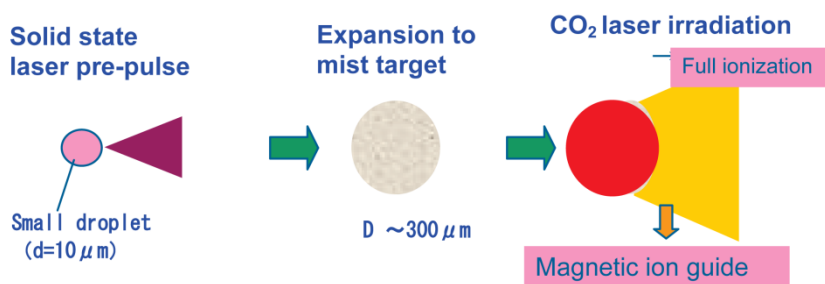


Fig. 1. Schematic of Tin plasma by double pulse method

The conversion efficiency (CE), from the input laser pulse energy to the generated EUV pulse energy at 13.5nm (2% bandwidth,  $2\pi$  sr), is the major parameter for improvement in high average power EUV light source for better economy. Low repetition rate pulsed CO<sub>2</sub> laser was composed of transverse discharge modules, and often employed in laser plasma

experiments until 90's, but gradually disappeared from laboratories after improvements of solid state pulsed lasers. It was once employed as a driver of a plasma X-ray laser from a carbon target (Suckewer, et.al., 1983).

Medium average power pulsed CO<sub>2</sub> laser systems are very successful tools for various applications ranging from material processing of metals, glass, ceramics and epoxy, paint removal and medical or spectroscopic applications, to the generation of laser produced plasmas as UV, EUV and soft X-ray sources. One drawback is the limited repetition rate of TEA CO<sub>2</sub> laser based source, another drawback is limited controllability of the pulse width in low pressure microwave excited lasers. Attempts were reported in early 90's to operate microwave excited CO<sub>2</sub> laser modules in a Q-switched oscillator mode of CW 2kW device (Sakai et.al., 1994) and an oscillator-amplifier mode of CW 7kW system (Bielech et.al., 1992). Typical performances were at the repetition rate of 4 kHz with output average power of 680 W with pulse energy of 170 mJ and pulse width in full width half maximum (FWHM) of 250 ns, and at the repetition rate of 10 kHz with average power of 800W, with pulse energy of 70 mJ, and 35 ns pulse width, respectively. Laser extraction efficiencies, however, were not very high in both cases in the short pulse mode. Commercially available short pulse CO<sub>2</sub> laser oscillator was known typically as EOM-10 from De Maria Electro Optics Systems, Inc (now Coherent Inc). The specification was average power of 10W at 100 kHz repetition rate with 15ns pulse width. The design guideline of a multi kW short pulse CO<sub>2</sub> laser system is characterized by high repetition rate, high pulse energy, high amplification efficiency and high beam quality. The system is based on commercial high average power CW CO<sub>2</sub> laser modules as amplifiers.

A short pulse oscillator was installed in our laboratory as the seeder for the amplifiers. The laser was an EO Q-switched, pulse length of 15~30 ns, single P(20) line, RF pumped waveguide CO<sub>2</sub> laser with 60 W output at a repetition rate of 100 kHz. The repetition rate was tunable as 10~140 kHz. Commercial 5 kW and 15 kW CW CO<sub>2</sub> lasers were employed as amplifiers. Every unit was 13.56 MHz RF-excited, fast axial flow lasers from Trumpf Inc. Lasers were modified as amplifiers by replacing both cavity mirror with ZnSe windows. The 5 kW laser used a standard gas composition of CO<sub>2</sub>:N<sub>2</sub>:He=5:29:66 at 120 Torr gas pressure. The axial gas flow speed was sufficiently high to keep the laser gas temperature low inside the operational condition. The length of a single gain region was 15 cm, and 16 cylindrical gain regions were connected in series in one laser unit; the tube inner diameter was 17mm. The total length of the optical pass inside the laser was 590 cm. The laser operated at 5 kW CW output power with a M<sup>2</sup> =1.8 beam quality. The electrical input power was 36 kW. The 15 kW laser as the main amplifier, used a standard gas composition of CO<sub>2</sub>:N<sub>2</sub>:He=2:10:48 at 150 Torr gas pressure. The length of a single gain region was 28 cm, and 16 active cylindrical gain regions were connected in series; the tube inner diameter was 30 mm. The total length of the optical pass inside the laser was 890 cm. The maximum electrical input power was 88 kW. The key parameters of the amplifier are the extraction efficiency and beam quality. A series of experiments were performed to clarify these parameters to estimate the final possible values (Hoshino et.al., 2008).

The experimental setup is shown as Fig.2 with expected output power of 10kW. The maximum average output power of 8 kW was experimentally obtained at a repetition rate of 100 kHz with 3kW input power to the main amplifier. Parasitic oscillations and/or optical coupling between amplifier modules were not significant in burst mode. It was successful to extract 5kW power in pulsed mode from CW 15kW laser. The extraction efficiency (output power-input power/ CW output power) was over 30%. Initial estimation of extractable

power from the main amplifier was 7kW, but the experimentally obtained power of 5kW indicated many factors for further improvement.

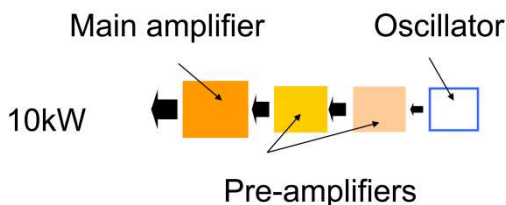


Fig. 2. Schematic diagram of multi stage MOPA, short pulse CO<sub>2</sub> laser

The laser beam quality was measured with a ZnSe lens of 508mm focal length and a slit-scan type beam profiler (Photon Inc., NanoScan). The laser beam size at the lens focus was measured for the oscillator and amplifier, resulting in a beam quality factor  $M^2$  as 1.1. Especially, the laser beam size was identical before and after amplification, i.e. the amplification did not cause any phase distortion. Fig.3 shows a typical spatial beam profile. Fig.4 shows the temporal laser pulse profile of the amplified laser output. The pulse duration was 20 ns (FWHM) and the pedestal was below 10% of the total pulse energy. A pedestal and/or tail of the seed laser pulse could be amplified and reduce the laser gain. Back scattering light from Tin mist target is experimentally less than 10% of the input laser energy, and backward amplification must be carefully avoided by full depletion of residual laser gain.

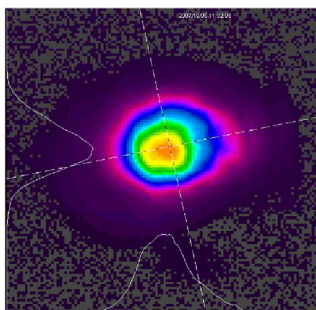


Fig. 3. CO<sub>2</sub> laser beam of  $M^2=1.1$

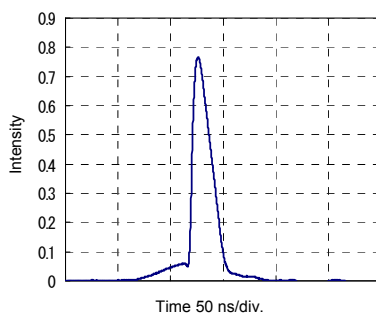


Fig. 4. CO<sub>2</sub> laser pulse with low pedestal

### 2. 10ns, 100 kHz operation of CO<sub>2</sub> laser at 10kW average power

CO<sub>2</sub> molecular dynamics is the fundamental subject to understand the operational parameters of pulsed CO<sub>2</sub> laser. Figure 5 shows a typical energy diagram of CO<sub>2</sub> laser active medium.

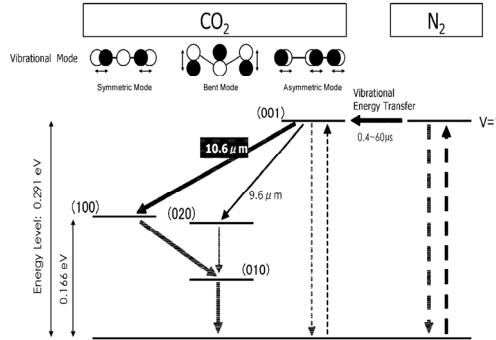


Fig. 5. Energy level diagram of active CO<sub>2</sub> laser medium

Short pulse, high repetition operational CO<sub>2</sub> laser is the most suitable laser technology to meet the requirements of HVM EUV source. Free electron lasers (FEL) are also capable of realizing high average power, short pulse coherent beam, based on the emerging superconducting energy recovery linac (sERL) technology (Krafft, 2006). However, the pulse energy is in sub mJ range with a few ps pulse width at 75MHz repetition rate, which does not match to the plasma production specifications for EUV sources.

Short pulse CO<sub>2</sub> laser technology was well studied by TEA discharge oscillator-amplifier configuration up until the 1990's (Decker, et.al, 1991). There were two major limitations on this scheme, namely, a low repetition rate up to 10Hz and backscatter amplification in non-saturated amplifier medium. The gain medium in the RF pumped CO<sub>2</sub> laser is a CO<sub>2</sub>/N<sub>2</sub>/He mixture of typically 100 Torr pressure. The CO<sub>2</sub> molecule stores energy in the rotational-vibration mode from electric collision excitation in the 00<sup>0</sup>1 band, and the typical relaxation time for the vibration is 0.5μsec, which is shorter than the pulse interval time of 10μsec for 100kHz repetition rate. The amplification that is described in this case is short pulse amplification and expressed by the Frantz-Nodvik equation (Rheaut, et.al, 1973), where  $E_{in}$  is the input fluence in mJ/cm<sup>2</sup>,  $E_{out}$  is the output fluence,  $E_s$  is the saturation fluence,  $g_0$  is the small signal gain coefficient in cm<sup>-1</sup>,  $L$  is the gain medium length in cm. Maximum available fluence after single pass amplification  $E_m$  is given by  $g_0 \cdot L \cdot E_s$  in mJ/cm<sup>2</sup>.  $g_0$  and  $E_s$  are functions of medium parameters proportional to the upper state molecule numbers as,  $\sigma N^*$ , and inversely proportional to the radiative cross section as  $h\nu/2\sigma$ , each other. The Frantz-Nodvik equation describes the short pulse amplification as,

$$E_{out} = E_s \cdot \ln[1 + \exp(g_0 \cdot L)[\exp(\frac{E_{in}}{E_s}) - 1]] \tag{1}$$

and the equation is valid provided that the pulse duration  $\tau_p$  is long compared to the rotational relaxation time  $\tau_r$ , or short, namely in the case of  $\tau_p \gg \tau_r$  or  $\tau_p \ll \tau_r$ . CO<sub>2</sub> laser amplification in the intermediate region, namely in the case  $\tau_p \approx \tau_r$ , is treated by rotational reservoir model calculations, which requires non practical numerical solutions (Harrach,

1975). The rotational relaxation time is calculated as  $\tau_r = 2.3\text{ns}$  for 100 Torr and a 450°C medium, while the typical laser pulse width in the example is  $\tau_p = 15\text{ns}$ . The characteristic number  $\tau_p / \tau_r$  is 6.5 for 100 Torr medium, and the work of F.Rheaut deals with the case of almost the same ratio for 1 atmosphere.

As a parameter study, small signal gain coefficient  $g_0$  is tentatively assumed as 1%/cm, and the saturation fluence is as 10mJ/cm<sup>2</sup> for a 100 Torr RF pumped CO<sub>2</sub> laser amplifier. The maximum fluence  $E_m$  is then given as 10mJ/cm<sup>2</sup> for L=1m gain length. Figure 6 shows one early experimental result of 15ns pulse amplification at 100 kHz of an axial flow CW 15kW laser. The average beam diameter was  $\sim 15\text{mm}$ , and amplification parameters were calculated as  $g_0=0.43\%/cm$ , and  $E_s=8.0\text{mJ/cm}^2$ , by numerical fitting of the experimental data to the equation (1). The fitting gave reasonable results in spite of the  $\tau_p \gg \tau_r$  condition (Ariga, 2007). It was concluded that the Frantz-Nodvik equation was practically usable in this semi-intermediate region for characterization of the amplifier parameters. It seems reasonable by accounting the measured  $E_s$ , together with an effort to increase  $g_0$  to 1%/cm, to obtain 100mJ pulse energy from the amplifier once the gain cross section A is 10cm<sup>2</sup>, or the gain length L is 10m with A=1cm<sup>2</sup>. The cross section A is depending on the amplifier design, and the gain length L is limited by self oscillation of the amplifier.

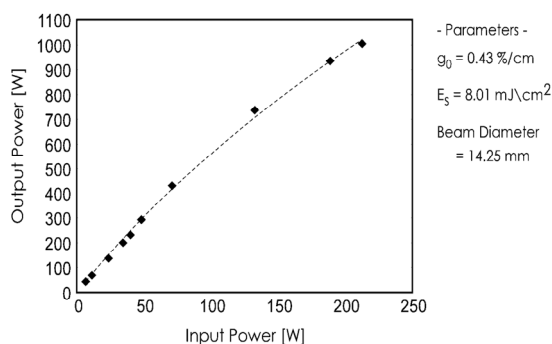


Fig. 6. Short pulse amplification data of 15kW CW output power module with 15ns pulse width at 100 kHz. The results were best fitted by the Frantz-Nodvik equation to give the effective value of  $g_0$  and  $E_s$ .

A short pulse amplifier is characterized by its medium gain diameter, D and gain length, L. The most common limitation of the available gain is set by the amplified spontaneous emission (ASE) on the optical axis, which deteriorates the pulse signal to noise ratio (SN), and depletes the available gain. A general mathematical formula on this phenomenon has been reported by Lowenthal et.al. (Lowenthal et.al,1986). On axis ASE flux is given by equation (11) from this work, for the purpose of numerical calculation. Figure 16 of the paper shows the achieved  $g_0L$  with parameters L/D. It is generally advised to keep  $g_0L$  less than 3 for a single pass amplifier, especially for storage lasers which have no coherent flux to extract gain simultaneously with pumping (short pulse amplification in cw pumped medium). A short pulse CO<sub>2</sub> laser amplifier has a typical gain diameter of 1cm, an optical gain length of 1m and an aspect ratio L/D large enough to consider the configuration as one dimensional. The gain depletion effect is less significant compared to the cubic gain medium previously reported (Lowenthal, et.al. 1986), but the on axis ASE effect is similar. Parasitic

oscillation is experienced in actual experiments and this is often the practical limit for full amplification. The phenomena are strictly dependant on the device design, namely partial reflection from laser wall, optics holders or leakage through isolators. It is an issue to be treated for each laser system, but the physical fundamental is the same as the double pass case by Lowenthal et.al.

It is preferable to employ gaseous saturable absorbers like SF<sub>6</sub> in the multi stage amplifiers, to avoid damage to solid-state saturable absorbers like p-doped Germanium (Haglund, et.al. 1981). The typical switching threshold in the gaseous saturable absorbers is 10mJ/cm<sup>2</sup>. Also, the optical beam delivery system requires optimization to efficiently depress pulse pedestal. An electro optical switch, which uses solid-state material like CdTe, is employed in the lower average power stage to realize better noise depression (Slattery, et.al. 1975). The damage threshold is dependant on the laser parameters such as pulse width, fluence, average power and beam uniformity. Laser beam containing hot spots can cause damage to the material surface even at much lower fluence. Solid-state materials suffer stronger thermal lens effects as shown by the following formula (Koechner, 1999).

$$f = \frac{KA}{P_a} \left( \frac{1}{2} \frac{dn}{dT} + \alpha C_{r,\phi} n_0^3 + \frac{\alpha r_0 (n_0 - 1)}{L} \right)^{-1} \quad (2)$$

The first term is the temperature dependant refractive index change, the second term is stress induced refractive index change, and the final term is temperature dependant surface modification. Thermal lensing is the most significant phenomenon in the power amplifier stage with optical components, especially for ZnSe or Diamond windows. The effective focus depends on the beam power, and active feedback is necessary to realize stable beam propagation throughout the whole laser optical path. Figure 7 shows a model calculation of the thermal loading effect to the beam propagation through 2 stage amplifiers of axial flow type of 5kW CW output, with an input of pulses in 20ns at 100 kHz repetition rate input with 60W average power (Nowak, et.al, 2008).

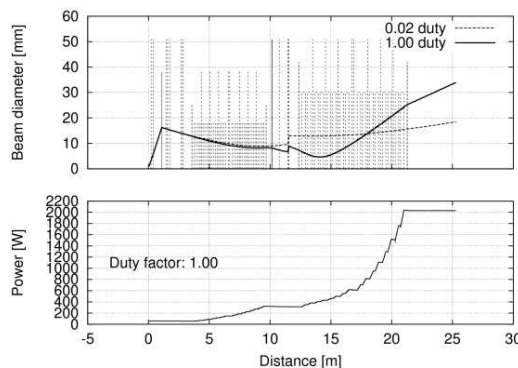


Fig. 7. Calculated results of the amplified beam diameter behavior depending on the operational duty. Input power is 60W at a distance of 0m, and the output optics of the first 5kW amplifier is at a distance of 10m. The input optics of the second module is at a distance of 11m. These windows suffer from strong thermal lensing effects which lead to beam diameter fluctuation.

It is indicated that the thermal lens effect is not deterministic at low duty operation (2%), but significant at 100% duty operation. Filling factor  $\Phi$ , is the parameter used to measure the usability of the gain region by the propagating beam,

$$\Phi = \text{beam volume} / \text{gain volume} \quad (3)$$

This is reduced at higher duty operation due to a shorter thermal lens focus length, and amplification saturation is lower at higher duty operation with reduced  $\Phi$ . Specifically designed active feedback control is necessary to stabilize the beam propagation at high duty operation. Figure 8 shows an experimental example of the beam diameter at the amplifier exit, with and without active beam control (Nowak, et.al, 2008). Lower spatial quality oscillator beam causes micro lens effects in the transparent optical components, and leads to chaotic beam amplification with a higher  $M^2$  number. Design of a controlled spectrum oscillator with high quality spatial profile is important for better amplified beam quality, and efficient amplification.

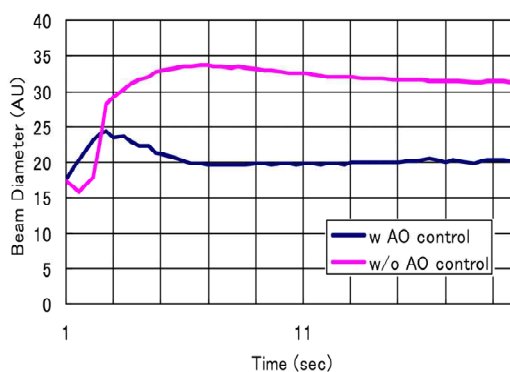


Fig. 8. Measured beam diameter after output window with and without active optical feedback.

### 3. New generation oscillator technologies

Precise control of the amplification depends on the quality of the oscillator pulse. Recent development of two different IR source technologies, namely OPA(Optical Parametric Amplifier) and QCL(Quantum Cascade Laser) are reviewed in this paragraph. Compact slab CO<sub>2</sub> laser is employed as the gain medium of regenerative amplifier to boost the weak initial IR beam. OPA and QCL are potentially controllable in its pulse width even in the pico second range.

Laser beam is characterized by its spectrum, and the low pressure CO<sub>2</sub> laser medium is composed of many vibration-rotational lines. The P(20) line is the single laser line in normal oscillation conditions at 10.6 $\mu$ m wavelength. The rotational relaxation time is calculated as  $\tau_r = 2.3$ ns for a 100 Torr and 450°C medium, which is not negligibly small compared to the typical laser pulse width  $\tau_p = 15$ ns. Electrically excited energy distributes in many other rotational modes of CO<sub>2</sub> molecules, and collisional relaxation to the P(20) line is limited

during the amplified pulse period. Figure 9 shows the spectrum structure of the laser lines, with a broad continuous spectrum from a solid state seeder overlapped, to fully extract the stored energy. Recent advanced nonlinear laser technology is at the stage of operating a broad band optical parametric oscillator (OPA) at the center wavelength of 10.6 $\mu\text{m}$ , with more than 10mW at 150kHz (Light Conversion, "ORPHEUS", 2011). This specification is enough to seed a single transverse mode CO<sub>2</sub> laser oscillator.

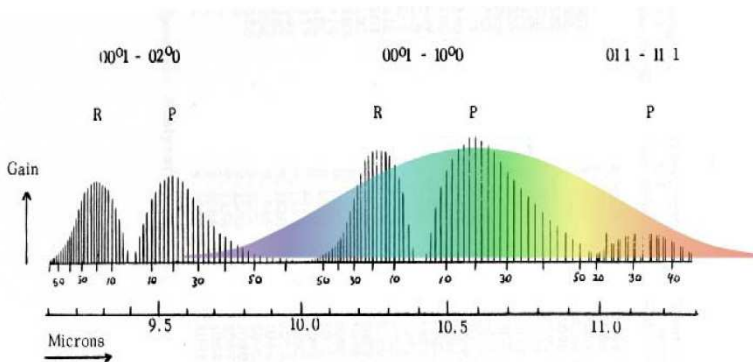


Fig. 9. CO<sub>2</sub> laser spectrum structure overlapped with a broad OPA seeder spectrum

Multiline amplification was calculated to evaluate the effectiveness of the low pressure CO<sub>2</sub> laser at 15kW CW output power. The beam diameter was assumed to be 18mm. Numerical result shows the amplification enhancement, with 4 lines composed of P(16,18,20,22) as 1.3 times higher than the single P(20) amplification case. Figure 10 shows the calculation result of the gain  $\Gamma$ . Emerging quantum cascade lasers (QCL) are available, which can generate specific lines of the P band of the CO<sub>2</sub> laser (Cascade Technologies, LS03D, 2009) and possibly seed a CO<sub>2</sub> laser oscillator with a discrete spectrum. QCL lasers are thus ideal as compact and robust seed sources. They can be accurately tuned to particular gain lines of the CO<sub>2</sub> medium with sufficient accuracy. QCL lasers are capable of tens of mW output power at typical pulse durations of 10ns, providing good bandwidth matching to a lasing line in a typical CO<sub>2</sub> medium. A QCL can provide at least 3 orders of magnitude higher power per self oscillation lines of a small oscillator, thus relaxing the requirement of the roundtrip gain and the number of roundtrips in the seeded oscillator, thereby improving power output and stability. The theoretical prediction of Fig.10 was recently confirmed by QCL multiline seeded pulses in a large slab amplifier (Nowak, 2011).

Multiline amplification effectively enhances small signal gain  $g_0$  compared to CW gain, and saturation fluence  $E_s$ , by improving the spectrum factor, and this leads to the enhancement of maximum available flux  $E_m$ . The final optical limit, typically 1J/cm<sup>2</sup>, is given by the optical damage of the output window, which is more than one magnitude higher than the available  $E_m$ . The small signal gain  $g_0$  and saturation fluence  $E_s$  are the two basic parameters to characterize for any amplifiers (DeaAutels, et.al. 2003). It is reasonable to expect double enhancement of  $E_m$  to 20mJ/cm<sup>2</sup> after optimization of amplifier parameters, and the available beam energy as 200mJ with the effective gain volume as  $LA = 1000 \text{ cm}^3$  (1 liter). Typical repetition rate of 100 kHz gives the average output power as 20kW, after meeting all requirements described in this article.



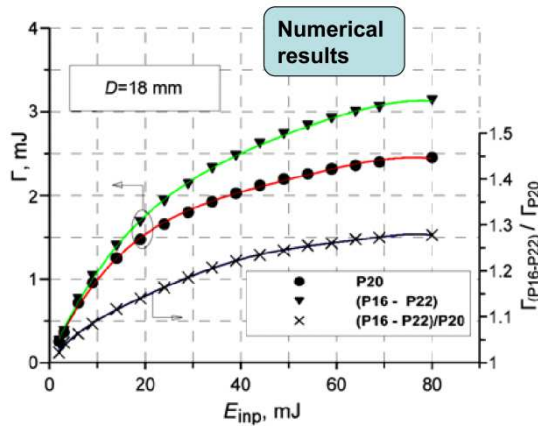


Fig. 10. Absolute (●▼) and relative (X) energy extraction from a main amplifier tube pumped by a CW RF discharge with discharge power 88 kW. The input beam shape is Gaussian with diameter D=18mm. The energy extraction is plotted to the input pulse energy. The symbol -X- is the relative gain ratio of single P20 line to 4 lines (P16-P22) amplification

#### 4. Further developments

It is understood that the high conversion efficiency of EUV light comes from the UTA (unresolved transition arrays) of highly ionized high Z plasma. The peak wavelength of the UTA is depending on the Z number, and further shorter wavelength plasma has a similar physical behavior (Li, et.al. 2011). The first generation EUV source at 13.5nm wavelength works well up to 11nm node of semiconductor mass production within the next one decade. A possibility to switch to a shorter wavelength (BEUV: beyond EUV) is required to be studied in advance (Banine, et.al, 2010). Availability of high reflectivity mirror at 6.x nm region initiated basic research to find candidate heavy elements with high UTA emission in this wavelength region (Churilov, et.al, 2009). Intensive research has revealed that the UTA emission has peak intensity from Gadolinium at 6.7nm wavelength comparably efficient to that of Tin at 13.5nm. Lower density plasma is favorable for less opacity effect, and short pulse CO<sub>2</sub> laser is again the best driver (Higashiguchi et.al, 2011). The optimum plasma temperature increases from 40eV for Sn at 13.5nm, to 150eV for Gd at 6.x nm. The laser plasma temperature is expressed as

$$T \propto (I_0 \lambda^2)^{2/3} \tag{4}$$

where I<sub>0</sub> is the laser peak intensity, and λ is the laser wavelength (Ramis et.al, 1983). It is understood that a short pulse CO<sub>2</sub> laser is better fitted to higher plasma temperature due to its longer wavelength. Optimum laser pulse width for highest CE for Sn at 13.5nm is typically 15nsec, but higher temperature Gd plasma dissipates faster, and shorter pulse length may be required for highest CE. Minimum sustainable pulse width in low pressure CO<sub>2</sub> laser amplifier is estimated from rotational gain bandwidth Δν(Abrams, 1974) as,

$$\Delta\nu = 7.58 ( \varphi_{CO_2} + 0.73\varphi_{N_2} + 0.64\varphi_{He} ) \times P(300/T)^{1/2} \tag{5}$$

where  $\phi$  is the partial ratio of each component gas, P is the total pressure in Torr, and T is the gas temperature in K.  $\Delta\nu$  is given as

$$\Delta\nu = 424 \text{ MHz} \quad (6)$$

for typical gas parameters as

$$\text{CO}_2 : \text{N}_2 : \text{He} = 1:1:8$$

$$P = 100 \text{ Torr} \quad (7)$$

$$T = 450 \text{ K}$$

The minimum pulse width is estimated from the Fourier transform limit of a Gaussian pulse as

$$\Delta\nu \cdot \Delta t = 0.44 \quad (8)$$

and the resulting  $\Delta t$  is around 1 nsec. The present oscillator is a QCL seeded Q-switched, cavity dumped laser based on a RF pumped low pressure CO<sub>2</sub> laser. Typical output pulse width is 15nsec at 100 kHz repetition rate with 5W average power. Shorter pulse width is available by various methods like electro-optical or laser pulse slicing, depending on the requirement from future plasma experiments. Careful optical design of amplifiers can sustain the amplified pulse width for the requirement by dispersion compensation.

Another important field where 10 $\mu\text{m}$  wavelength is effective for short wavelength light generation, is the laser Compton X-ray generation. It is already well studied on the optimization of the laser-Compton hard X-ray source by single shot base (John, 1998, Endo, 2001). Experimental results agreed well with theoretical predictions. Highest peak brightness is obtained in the case of counter propagating laser pulse and electron beam bunch, in the minimum focusing before nonlinear threshold. The new short wavelength light source is now well matured to demonstrate single-shot phase contrast bio imaging in hard X-ray region (Oliva, et.al, 2010).

The major challenge of the laser Compton source in the EUV/SXR region is the lower electron beam voltage, which in turn results in a larger interaction cross section. Figure 11 describes the schematic of the laser-Compton interaction between electron beam and laser.

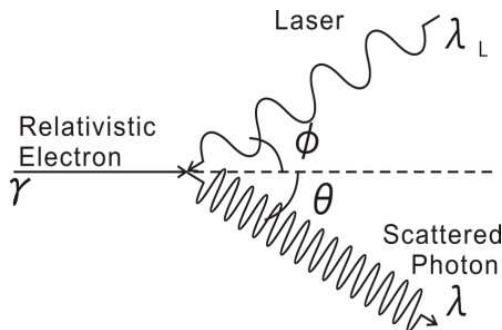


Fig. 11. Schematic of laser-Compton scattering process

Laser-Compton scattering photon spectrum has a peak in the forward direction at a wavelength;

$$\lambda_p = \frac{\lambda_L \left(1 + \frac{K^2}{2}\right)}{2\gamma^2(1 + \beta \cos\phi)} \quad (9)$$

where  $\gamma$  and  $\beta$  are Lorentz factors,  $\lambda_L$  the laser undulation period (laser wavelength),  $K$  the  $K$  parameter of the undulator which is equivalent to the laser intensity parameter, and  $\Phi$  the colliding angle. The spectrum depends on the angular distribution; the wavelength  $\lambda$  is emitted at

$$\theta = \frac{1}{\gamma} \sqrt{\frac{\lambda - \lambda_p}{\lambda_p}} \quad (10)$$

It is seen that higher  $\gamma$  electron beam produces less divergent light. Figure 12 shows the relationship between electron beam energy and maximum (forward) photon energy for both laser wavelengths by Nd:YAG laser (1.06 $\mu$ m) and CO<sub>2</sub> laser (10.6 $\mu$ m). As a result of Fig. 12, the required electron beam energy is 3.2MeV (1.06 $\mu$ m) and 10.2MeV (10.6 $\mu$ m) in order to produce 6.7nm SXR. It makes large difference to treat such a low energy electron beam. The Lorentz factor  $\gamma$  is 6.3 and 20.0, respectively, which means 3 times better directivity with 10.6 $\mu$ m laser than that of 1.06 $\mu$ m.

The general formula of obtainable photon flux  $N_0$  is calculated in the normal collision by the following expression.

$$N_0 \propto \frac{\sigma_c N_e N_p}{4\pi r^2} \quad (11)$$

where  $\sigma_c$  is the Compton cross section ( $6.7 \times 10^{-25}$  cm<sup>2</sup>),  $N_e$  the total electron number,  $N_p$  the total photon number, and  $r$  the interaction area radius.

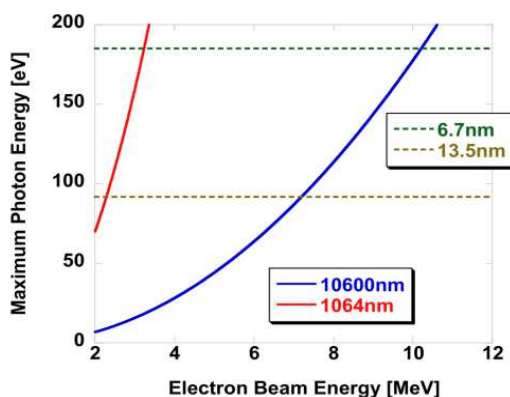


Fig. 12. Laser-Compton photon energy vs electron beam energy. Comparison 1064nm (Nd:YAG) with 10600nm (CO<sub>2</sub>) wavelength as the photon target.

It is useful to calculate standard SXR photon numbers obtainable in ideal parameters in both cases. As described in Eq. (11), the SXR number is proportional to the laser photon number. The approach to increase the photon average flux is to increase  $N_e$ ,  $N_p$  and decrease  $r$ , but there are instrumental limitations to realize these simultaneously. The practical limitation of laser average power is determined by a damage on optical components, which is determined by average and peak intensity ( $W/cm^2$ ). It is suggested that the usage of  $10.6\mu m$  CO<sub>2</sub> laser has an advantage to produce one order larger number of SXR photons by the same intensity compared with  $1\mu m$  solid state lasers. Another limitation is the onset of the nonlinear threshold of the higher harmonics generation, which is evident over  $10^{17}W/cm^2$  laser irradiation intensity (Kumita, 2008).

Usual approach is to increase the repetition rate of the event, and the obtainable photon average flux is expressed as;

$$N = f \times N_0 \quad (12)$$

where  $f$  is the repetition frequency. Characterization of the laser-Compton X-ray source has been undertaken with  $f$  as 1-10 Hz typically. High flux mode requires  $f$  in the range from kHz to MHz region.

It is under development of pulsed solid state laser storage in an optical super-cavity for laser-Compton X-ray sources (Sakaue, 2010, 2011). The enhancement inside the optical cavity was 600, in which the finesse was more than 2000, and the waist of  $60\mu m$  ( $2\sigma$ ) was stably achieved using a  $1\mu m$  wavelength Nd:Vanadium mode-locked laser with repetition rate 357MHz, pulse width 7ps, and average power 7W. Schematic of super-cavity is shown in Figure 13.

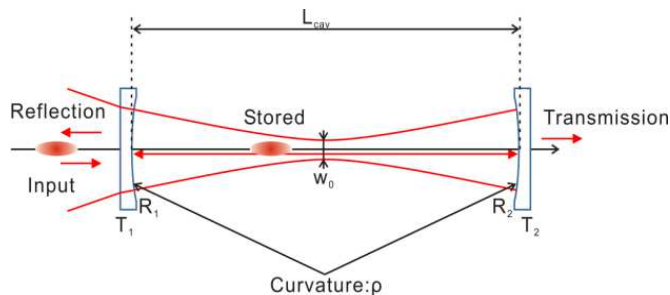


Fig. 13. Schematic of laser storage super-cavity.

Design and optimization is described here on a super-cavity for storing  $10.6\mu m$  CO<sub>2</sub> laser pulses. Super-cavity requires high reflectivity and high transmittance mirror i.e. ultra-low loss mirror as an input and high reflectivity mirror as an output for high enhancement. The enhancement is presented by using cavity finesse ( $F$ ) as (Hodgson, et.al, 2005);

$$S_{cav} = \frac{F}{\pi} \quad (13)$$

It is noted that the assumed cavity length is perfectly matched with input laser light. Finesse ( $F$ ) is given by;

$$F = \frac{\pi\sqrt{R_{eff}}}{1 - R_{eff}} \quad (14)$$

where  $R_{eff}$  is  $\sqrt{R_1 R_2}$ . As described above, higher reflectivity provides a higher enhancement super-cavity. Particularly, the loss, which includes both absorption and scattering, on the reflection coating is critical issue for storing a high power laser beam as described above. Such a high quality optical mirror was difficult for far infrared wavelength, however, there are now some products usable for super-cavity mirrors (Ophir Optics, 2009). Super-cavity for 10.6 $\mu$ m laser pulse can be achieved with the enhancement of about 600 by using best mirrors available. Figure 14 shows the calculated transmission, reflection and stored power of the super-cavity as a function of the phase advance in one cavity circulation i.e. super-cavity length. The dotted line shows the reflection/transmission from the cavity and the solid line is stored power inside the super-cavity, assuming as input power is 1. There is no transmission light because Mirror 2 transmission is 0%. The enhancement of 600 is achieved by this super-cavity. The precision of cavity length adjustment is one issue for stable operation. The requirement is one-order relaxed due to the wavelength in case of CO<sub>2</sub> laser, thus the stable operation with enhancement of 600 and more can be easily achieved from our experiences in 1 $\mu$ m laser storage. Critical issue for higher enhancement is to obtain the extremely low loss and high reflectivity mirrors, which is the key R&D of multi-layer coatings with high resistance substrates.

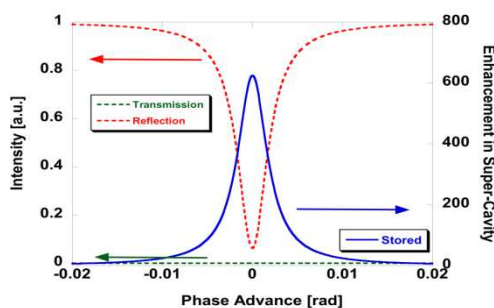


Fig. 14. Calculated results of CO<sub>2</sub> laser super-cavity as a function of phase advance in one revolution of cavity.  $2\pi$  phase advance corresponds to  $\lambda/2$  cavity length mismatch with the laser frequency.

Concerning a small waist achievement, our source requires 40 $\mu$ m waist (2 $\sigma$ ). The waist of super-cavity is described as;

$$w_0^2 = \frac{\lambda}{\pi} \frac{\sqrt{L_{cav}(2\rho - L_{cav})}}{2} \quad (15)$$

where  $\lambda$  is wavelength of laser,  $L_{cav}$  cavity length,  $\rho$  curvature of cavity mirror. While high enhancement is easier, small waist cavity is difficult for 10.6 $\mu$ m laser as described in Eq. (15). However the two-mirror, Fabry-Perot cavity would be difficult to achieve small waist due to the cavity structure is confocal, we are developing a concentric, four-mirror super-cavity (Y.Honda, et.al. 2009). This technique can reduce the mirror alignment requirements as two order magnitude. We estimate that 40 $\mu$ m waist can be achieved using concentric super-cavity.

The first preliminary experimental results were obtained by using a single transverse mode, CW 10W CO<sub>2</sub> laser in a two mirror super cavity (Sakaue, et.al. 2011). The reflectivity of the input mirror was 99.5% with 15m curvature, and the CW CO<sub>2</sub> laser was operated with 10W maximum power of single longitudinal mode. The obtained transmitted light is shown on the oscilloscope with a sweeping voltage signal to the Piezo driver. The highest peak signal corresponds to the fundamental transverse mode, followed by higher spatial modes. The measured Finesse was around 300, which is almost half of the calculated value 624. Measured beam waist was 2.1mm, compared to the calculated value 1.8mm. The experiment showed a relatively stable result of the optical storage cavity in the CO<sub>2</sub> laser wavelength. Next step is planned as a demonstration of the optical storage cavity with picosecond pulses.

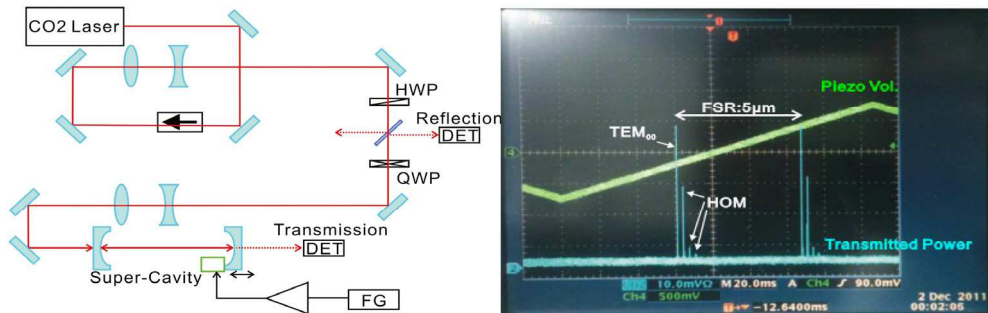


Fig. 15. Experimental setup and first result of CO<sub>2</sub> laser storage. Signal train corresponds to the transmission light with cavity length interval of 5  $\mu\text{m}$ .

## 5. Conclusion

High average power, short pulse width CO<sub>2</sub> laser is originated in the EUV light source research in the beginning, but expanding its application to universal short wavelength plasma and non plasma sources. Reliable gas laser amplifiers with various geometrical structures are now employed with advanced solid state, semiconductor seeders to control its wavelength more precisely, and with advanced optics to enhance its pulsed average power to unprecedented level.

The author deeply expresses his thanks to his colleagues in the trials of research and development in EUV program. Early study on the CO<sub>2</sub> laser technology was successfully driven by Dr. T. Miura. He contributed also in the application of OPA technology as the broadband seeder for CO<sub>2</sub> laser oscillators. QCL was successfully studied as a seeder for precision control of the lasing lines by Dr. K. M. Nowak. Dr. H. Mizoguchi of Gigaphoton Inc. kindly gave me a chance to write this overview. The author deeply appreciates co-workers in Waseda University, especially Dr. K. Sakaue and Professor M. Washio in the CO<sub>2</sub> laser super-cavity program.

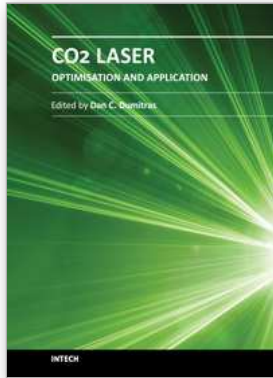
## 6. References

Abrams, R.L 1974 Broadening coefficients for the P(20) laser transition; Appl.Phys.Lett. 25, pp609-611

- Ariga, T. 2007 Development of a short pulse and high average power CO<sub>2</sub> laser for EUV lithography, Proc.SPIE 6346 634604 "XVI International Symposium on Gas Flow, Chemical Lasers and High Power Lasers", 4-8 September, 2006, Gmunden Austria
- Banine, V. Y., Koshele, K. N., Swinkels, G.H.P.M. 2011. Physical processes in EUV sources for microlithography J.Phys.D.App.Phys. 44 253001
- Bielesch, U., Budde, M., Fischbach, M., Freisinger, B., Schaefer, J. H., Uhlenbusch, J. and Viol, W. 1992 Q-switched multi kilowatt CO<sub>2</sub> laser system excited by microwaves, *Proceedings of SPIE 9th International Symposium on Gas Flow and Chemical Lasers*, pp57- 60 SPIE1810 ISBN: 9780819410108, August 1992, Heraklion, Greece
- Churilov, S. S., Kildiyarova, R. R., Ryabtsev, A. N. and Sadovsky, S. V. 2009 EUV spectra of Gd and Tb ions excited in laser-produced and vacuum spark plasmas Phys.Scr. 80 045303
- DeaAutels, L.G., Daniels, D., Bagford, J.O., Lander, M. 2003 High power large bore CO<sub>2</sub> laser small signal gain coefficient and saturation intensity measurements J.Opt.A:Pure Appl.Opt.5 pp96-101
- Decker, J.E., Lagace, S., Berube, J., Beaudoin, Y., Lin, S.L. (1991); Stable operation of a powerful 3-Hz line tunable TEA CO<sub>2</sub> oscillator-amplifiers system, Appl.Optics 30 pp1888-1890
- Endo, A. (2010); CO<sub>2</sub> laser produced Tin plasma light source as the solution for EUV lithography, InTech
- Endo, A.; Hoshino, H.; Ariga, T. & Miura, T. (2006). High power pulsed CO<sub>2</sub> laser for EUV lithography, *EUV Source Workshop*, May 2006, Vancouver, B.C. Canada, International Sematech
- Haglund, R.F., Nowak, A.V., Czuchlewski, S.J. (1981); Gaseous saturable absorbers for the helios CO<sub>2</sub> laser system, IEEE Quantum Electron. QE17, pp1799-1808
- Harrach, R.J. (1975); Effect of rotational and intramode vibrational coupling on short pulse amplification in CO<sub>2</sub>, IEEE J.Quantum Electron. QE-11, pp349-357
- Higashiguchi, T., Otsuka, T., Yugami, N., Jiang, W., Endo, A., Li, B., Kilbarr, D., Dunne, P., O'Sullivan, G. (2011) Extreme ultraviolet source at 6.7nm based on a low-density plasma, Appl.Phys.Lett. 99, 191502, 2011
- Hodgson, N. & Weber, H. (2005). *Laser resonators and beam propagation: Fundamentals, Advanced Concepts and Applications 2<sup>nd</sup> edition*, ISBN-10: 0387400788, Springer, Berlin
- Honda, Y., Shimizu, H., Fukuda, M., Omori, T., Urakawa, J., Sakaue, K., Sakai, H., Sasao, N. (2009) Stabilization of a non-planar optical cavity using its polarization property, Opt.Commun. 282 pp3108-3112
- Hoshino, H.; Suganuma, T.; Asayama, T.; Nowak, K.; Moriya, M.; Abe, T.; Endo, A. & Sumitani, A. (2008). LPP EUV light source employing high power CO<sub>2</sub> laser, *Proceedings of SPIE Emerging Lithography*, vol.6921, ISBN: 9780819471062, San Jose, CA, February, 2008, SPIE
- Koehner, W. (1999); *Solid-State Laser Engineering*, Springer, Berlin
- Koehner, W. (1999); *Solid-State Laser Engineering*, Springer, Berlin
- Kraft, G.A. (2006) Performance achievements and challenges for FELs based on ERLs FEL2006, TUAAU01, Aug 29, Berlin Germany
- Kumita, T., Kamiya, Y., Babzien, M., Ben-Zvi, I., Kusche, K., Pavlishin, I., V. Pogorelsky, I. V. Siddons, D. P. Yakimenko, V. Hirose, T. Omori, T. Urakawa, J. Yokoya, K. Cline, D. and Zhou, F. (2008) Observation of the Nonlinear Effect in Relativistic Thomson
- Li, B., Endo, A., Otsuka, T., O'gorman, C., Cummins, T., Donnelly, T., Kilbane, D., Jiang, W., Higashiguchi, T., Yugami, N., Dunne, P., O'Sullivan, G. (2011) Scaling of laser produced

- plasma UTA emission down to 3 nm for next generation lithography and short wavelength imaging, *Proceeding of SPIE Optics+Photonics* vol.8139, San Diego,CA, August 2011
- Lowenthal, D.D. Egglestone, J.M. (1986); ASE effects in small aspect ratio laser oscillators and amplifiers with nonsaturable absorption, *IEEE J. Quantum Electron.* QE-22, pp1165-1173
- Nowak, K.M.; Sukanuma, T.; Endo, A.; Sumitani, A.; Goryachkin, D.A.; Romanov, N.A.; Sherstobitov, V.E.; Kovalchuk, L.V.; Rodionov, A.Y. (2008). Efficient and compact short pulse MOPA system for laser-produced-plasma extreme-UV sources employing RF-discharge slab-waveguide CO<sub>2</sub> amplifiers, *Proceedings of SPIE High-Power Laser Ablation*, vol.7005, ISBN: 9780819472069, Taos, NM, April 2008, SPIE
- Nowak, K.M. (2011). Towards 20kW CO<sub>2</sub> laser system for Sn-LPP EUV source, *2011 International Workshop on EUV and Soft X-Ray Sources*, Dublin, Ireland November 7-9, 2011
- Oliva, P. Carpinelli, M. Golosio, B. Delogu, P. Endrizzi, M. Park, J. Pogorelsky, I. Yakimenko, V. Williams, O. Rosenzweig, J (2010), Quantitative evaluation of single-shot inline phase contrast imaging using an inverse Compton x-ray source, *Appl. Phys. Lett.* 97, 134104
- Ramis, R (1983) Electron temperature versus laser intensity times wavelength squared: a comparison of theory and experiments, *Nucl. Fusion* 23739
- Rheault, F. Lachambre, J.L. Gilbert, J. Fortin, R. Blanchard, M (1973); Saturation properties of TEA-CO<sub>2</sub> amplifiers in the nanosecond pulse regime, *Opt. Commun.* 8, pp132-135
- Sakai, T. & Hamada, N. (1994). Q-switched CO<sub>2</sub> laser using intense pulsed RF discharge and high speed rotating chopper, *Proceedings of SPIE Gas Flow and Chemical Lasers: Tenth International Symposium*, vol.2502, pp. 25-30, ISBN: 9780819418609, Friedrichshafen, Germany, September 1994, SPIE
- Sakaue, K Araki, S Fukuda, M Higashi, Y Honda, Y Sasao, N Shimizu, H Taniguchi, T Urakawa, J and Washio, M (2011) Development of a laser pulse storage technique in an optical super-cavity for a compact X-ray source based on laser-Compton scattering, *Nucl. Instrum. Meth.* A637 S107-S111
- Sakaue, K Endo, A and Washio, M (2011) Development of a 10 $\mu$ m optical storage cavity, *2011 International Workshop on EUV and Soft X-Ray Sources*, Dublin, Ireland November 7-9, 2011
- Sakaue, K Washio, M Araki, S K Fukuda, M Higashi, Y Honda, Y Omori, T Taniguchi, T Terunuma, N Urakawa, J and Sasao, N (2009) Observation of pulsed x-ray trains produced by laser-electron Compton scatterings, *Rev. Sci. Instrum.* 80 123304 1-7
- Scattering of Electron and Laser Beams, *Laser Phys.* 16 pp267-271
- Slattery, J.E. Thompson, J.S. Schroeder, J.B. (1975); Thermal pulse damage thresholds in cadmium telluride, *Appl. Opt.* 14, pp2234-2237
- Suckewer, S.; Skinner, C.; Voorhees, D.; Milchberg, D.; Keane, C. & Semet, A. (1983). Population inversion and gain measurements for soft X-ray laser development in a magnetically confined plasma column, *IEEE-QE* 19 pp1855-1860
- Yorozu, M Yang, J Okada, Y Yanagida, T Sakai, F Ito, S and Endo, A (2003) Spatial beam profile of the femtosecond X-ray pulses generated by a laser-Compton scheme, *Appl. Phys.* B76 pp293-297





## **CO2 Laser - Optimisation and Application**

Edited by Dr. Dan C. Dumitras

ISBN 978-953-51-0351-6

Hard cover, 436 pages

**Publisher** InTech

**Published online** 21, March, 2012

**Published in print edition** March, 2012

The present book includes several contributions aiming a deeper understanding of the basic processes in the operation of CO<sub>2</sub> lasers (lasing on non-traditional bands, frequency stabilization, photoacoustic spectroscopy) and achievement of new systems (CO<sub>2</sub> lasers generating ultrashort pulses or high average power, lasers based on diffusion cooled V-fold geometry, transmission of IR radiation through hollow core microstructured fibers). The second part of the book is dedicated to applications in material processing (heat treatment, welding, synthesis of new materials, micro fluidics) and in medicine (clinical applications, dentistry, non-ablative therapy, acceleration of protons for cancer treatment).

### **How to reference**

In order to correctly reference this scholarly work, feel free to copy and paste the following:

Akira Endo (2012). High Average Power Pulsed CO<sub>2</sub> Laser for Short Wavelength Light Sources, CO<sub>2</sub> Laser - Optimisation and Application, Dr. Dan C. Dumitras (Ed.), ISBN: 978-953-51-0351-6, InTech, Available from: <http://www.intechopen.com/books/co2-laser-optimisation-and-application/high-average-power-pulsed-co2-laser-technology-for-short-wavelength-light-sources>

# **INTECH**

open science | open minds

### **InTech Europe**

University Campus STeP Ri  
Slavka Krautzeka 83/A  
51000 Rijeka, Croatia  
Phone: +385 (51) 770 447  
Fax: +385 (51) 686 166  
[www.intechopen.com](http://www.intechopen.com)

### **InTech China**

Unit 405, Office Block, Hotel Equatorial Shanghai  
No.65, Yan An Road (West), Shanghai, 200040, China  
中国上海市延安西路65号上海国际贵都大饭店办公楼405单元  
Phone: +86-21-62489820  
Fax: +86-21-62489821

© 2012 The Author(s). Licensee IntechOpen. This is an open access article distributed under the terms of the [Creative Commons Attribution 3.0 License](#), which permits unrestricted use, distribution, and reproduction in any medium, provided the original work is properly cited.